Aerodynamic calculation of wind impact on mobile radar antenna design

D. A. Solomatin[1*] and *S. A.* Shumskaia[1]

[1]Moscow Aviation Institute (National Research University), 4, Volokolamskoe Shosse, Moscow, 125993, Russian Federation

Abstract. In this work, the aerodynamic strength calculation of the radar station was carried out in 37 design cases in which the direction of the wind flow and the position of the antenna panel relative to the vehicle were varied. The vehicle and container were considered exclusively in the aerodynamic calculation for the calculation of air masses. For the most stressed cases, the static calculation was carried out and the critical stresses of the whole structure under study and the antenna panel structure separately were determined.

1 Introduction

The strength calculation is carried out taking into account the action of the load-bearing elements' own weight combined with the load from the limit wind flow, directed frontally in relation to the antenna array [1-3]. The maximum wind velocity in the calculation was taken as 52.9 m/s. Aerodynamic calculations were performed taking into account the influence of the location of the cabin under the action of wind loads at an angle to the antenna panel. The maximum critical cases for which the strength calculation was performed were determined [4-8].

The input data is based on the following conditions:

- operating and limiting ambient temperature +50 ºC,
- relative humidity of 40% at +50 $^{\circ C}$ and an atmospheric pressure of 630 mm m.th.
- average air velocity 30 m/s.

The supporting structures MR consist of the following main elements: vehicle, container, rack with sprayer MR.

Calculation cases for blowing out the original vehicle model with container in which the rack is located MR: fixes the position of the container vehicle and varies the position of the stand in relation to the front of the panel in relation to the container vehicle: 0°, 45°, 90°, 135°, 180°, then relative to each fixed position of the rack MR varies the position of the machine with the container relative to the machine front in relation to the wind direction: 0°, 45°, -45°, 90°, -90°, 135°, -135°, 180°. A total of 37 design cases were obtained, 37 design cases were investigated, of which the cases most loaded by the pressure acting on the panel were applied in a further study.

* Corresponding author: gxtl@mail.ru

 https://doi.org/10.1051/e3sconf/202340205003

Static strength calculations were performed using the Static Structural module in the Software Ansys Workbench. The solution is based on the assumption of linearly elastic material properties and small deformations. Transition to fluidity and formation of plastic deformations in metal or damage in composite elements is not allowed [9-13].

Calculations determine the stress-strain state of the antenna panel.

2 Calculation results

For the necessary reliability of the results obtained, the modelled calculation area was taken from the maximum height of the object in question h_{max}= 6.550 m. (Fig. 1). The calculation area is taken in the form of a parallelepiped with the object in question located in it in such a way that the distance from the object to the plane on the leeward side is $10h \sim 65.5$ m., the distance from the top to the top plane, the distance from the object to windward and the two planes in the direction of the wind load is $5h \sim 32.75$ m. for the transmitting post.

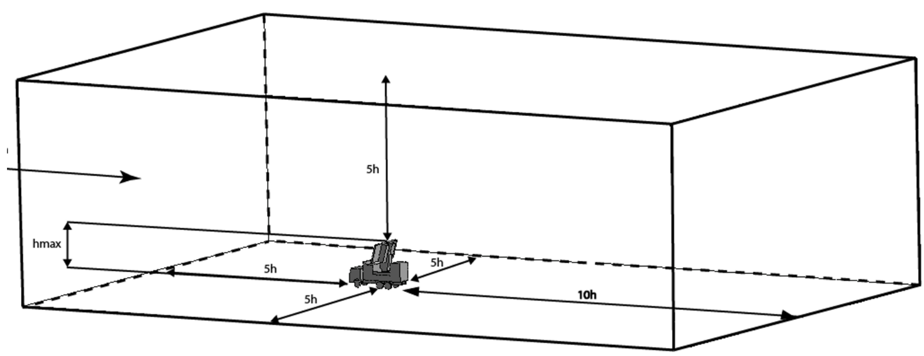

Fig. 1. Dimensions of the calculation area (h=6.550 m).

To obtain a more correct KE model, the calculation area in the vicinity of the object was divided into zones with different partitioning. For this purpose, 2 zones with a distance from the object of 2-4 m were modelled, Fig. 2.

 https://doi.org/10.1051/e3sconf/202340205003

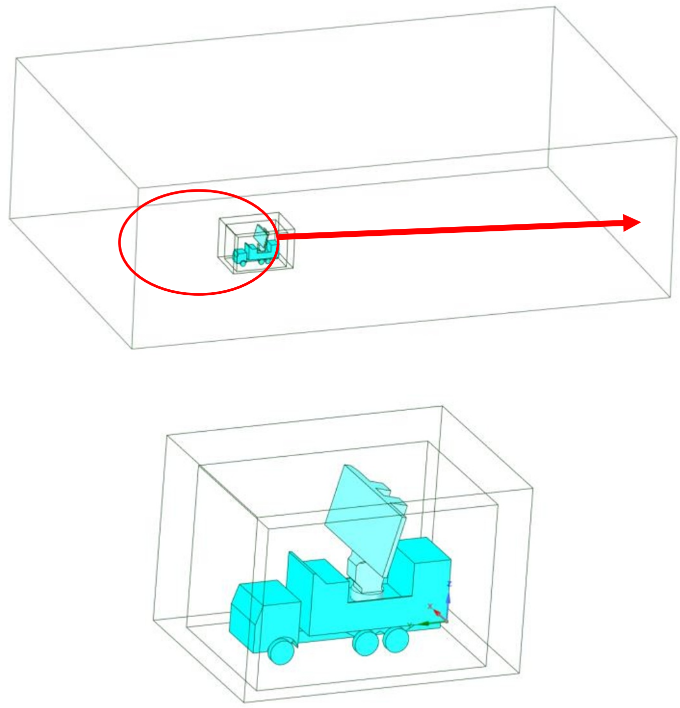

Fig. 2. Calculation area.

A tetrahedral mesh with element type Test 4 was used at the boundary and in the area closest to the post of the studied object, and at the distance with element type Hex 8. The finite element model of the computational domain is shown in Fig. 3, FEM consists of ~ 193103 elements and ~ 74001 nodes.

 https://doi.org/10.1051/e3sconf/202340205003

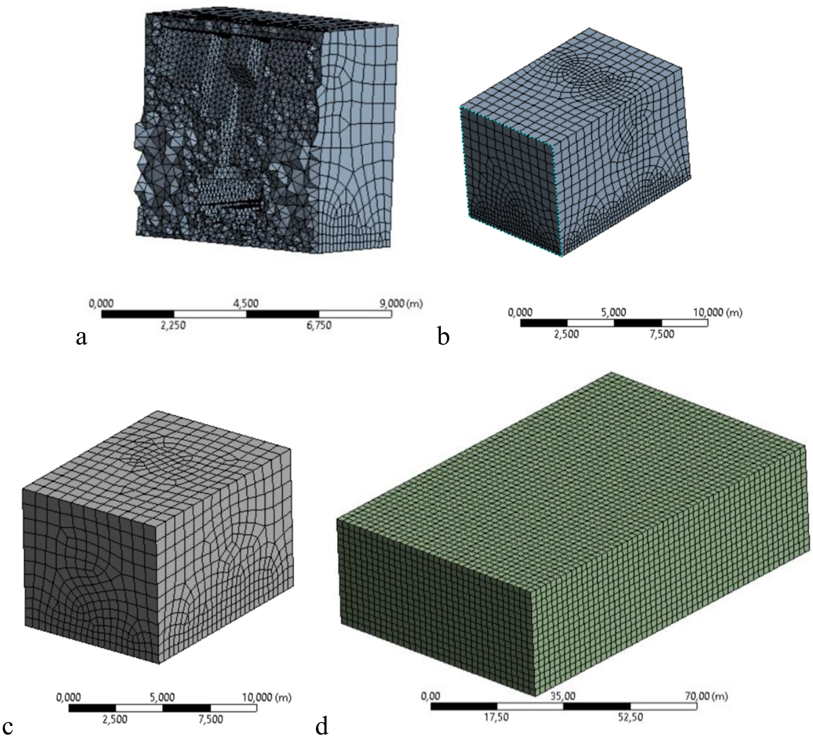

Fig. 3. FEM calculation area. (a - calculation area near the object under investigation in the cross section, b - calculation area of second approximation, c - calculation area of first approximation, d - calculation area at a distance from the object under investigation).

Based on the results, pie charts of "Wind Rose" (Fig. 4) of maximum pressure on the studied surface of the antenna panel depending on the direction of the airflow were plotted: 0°, 45°, -45°, 90°, -90°, 135°, -135°, 180°, relative to a container vehicle with a fixed rack position: 0°, 45°, 90°, 135°, 180°.

https://doi.org/10.1051/e3sconf/202340205003

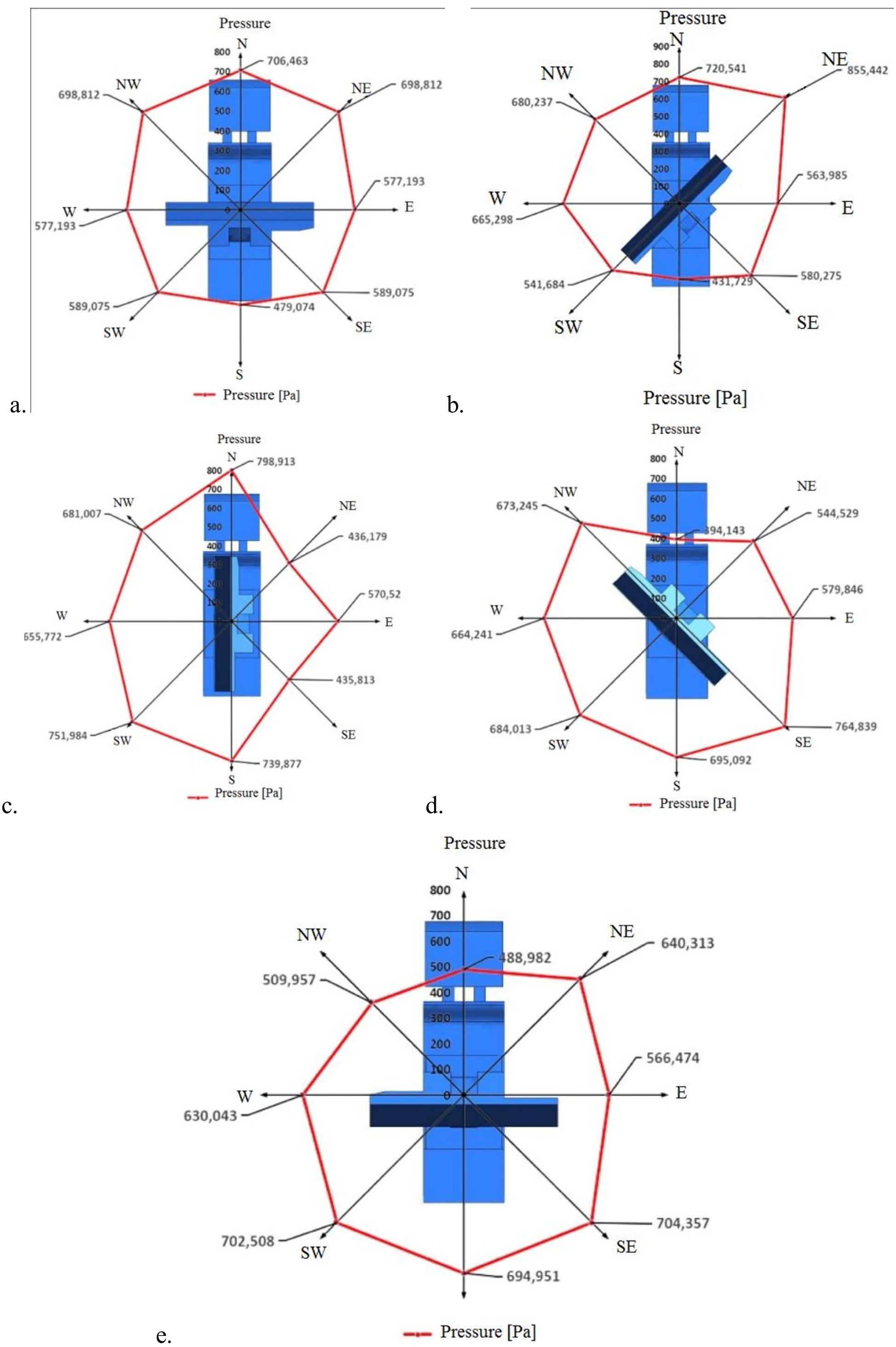

Fig. 4. Results of aerodynamic calculation (a - first design case of location MR; b – second design case of panel arrangement MR; c – third design case of panel location MR; d – fourth design case of panel location MR, e – fifth design case of panel location MR). Maximum operating pressure on the web MR was taken modulo the value.

The load-bearing metal structure of the antenna plate (1) is made in an I-beam profile with dimensions: length 5500 mm, height 55 mm, width 33 mm, wall thickness 3 mm. Antenna sublattice (2) consists of metal thin-sheet sections with thickness of 3 mm, which is a bent U-shaped profile with the following dimensions: length 2300 mm, width 125 mm, height 60 mm. Frame RD made of GRP pultrusion profiles (I-beams) with the following dimensions: length 2300 mm, width 20 mm, height 50 mm, wall thickness 2 mm. RD (4) modelled in 44 sections, each measuring 2300 mm long, 125 mm wide, 15 mm high.

The calculations are based on the standard characteristics of the materials used in the construction [14-37].

A grid with Tri3 element types and a predominance of Quad4 elements was constructed for the object under study. The finite element model of the calculated model is shown in Fig. 5, FEM consists of 566889 elements and 515937 assemblies.

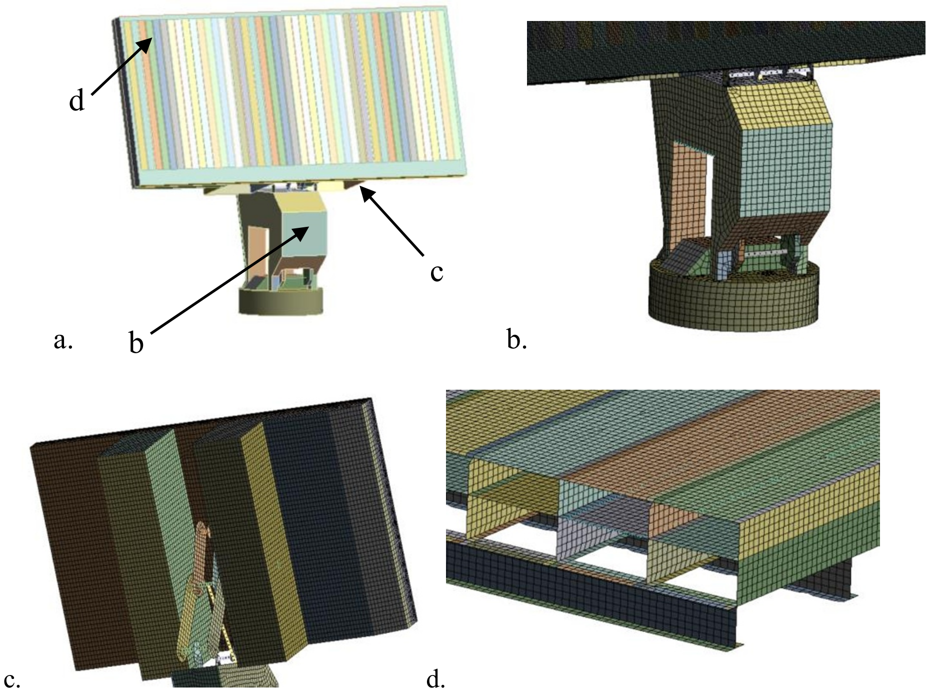

Fig. 5. Finite element model of the model to be calculated. (a - general geometry, b - struts, c - baskets, d - antenna web structures).

Standard material properties were used in the calculation. To account for the structure's own weight, gravity was taken into account by setting a condition of type (standard earth gravity) with an acceleration of gravity of 9.8 m/s^2. The condition for loading the antenna panel with wind flow was imported using a condition like (imported pressure). The setting of the boundary conditions is shown in Fig. 6.

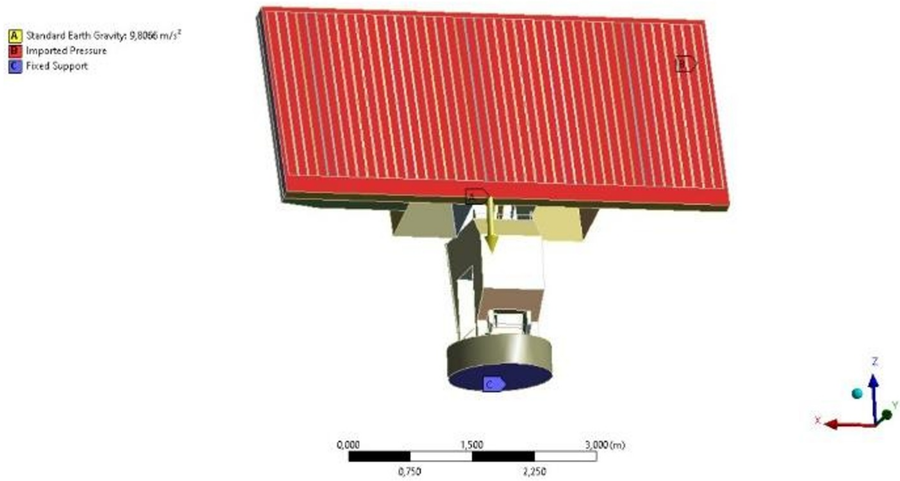

a.

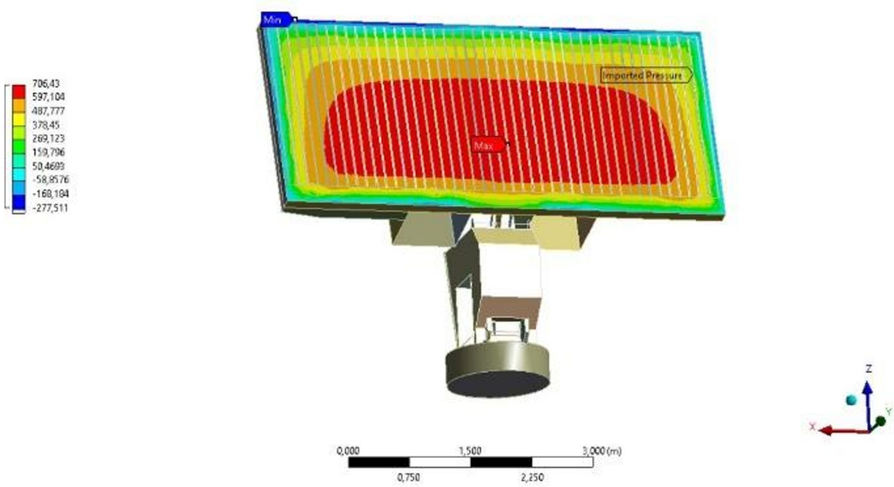

b.

Fig. 6. Boundary conditions of the calculation model (a - general boundary conditions, b - imported wind flow loading of calculation number 1).

The calculations take into account the condition of fixing the radar rack to the vehicle container with a boundary condition of type (fixed support) in the contact areas of the rack and the vehicle.

3 Conclusion

The calculations found the most stressed design cases, namely those with 45 degree wind direction and panel location - with pressure 720.541 [Pa], with 0 degree wind direction and panel location - with pressure 706.463 [Pa] and with 180 degree wind direction and 135 degree panel arrangement - with pressure 704.357 [Pa] in compression, with 45 degree wind direction and panel positioning - with pressure 855.442 [Pa] and with 90 degree wind direction, and panel position - with pressure 798.913 [Pa] on the tear-off. For the most stressed cases, the static calculation of the global structure as a whole has been carried out, taking into account the rigid fixing of the bottom surface of the bracket post, the load on the antenna panel obtained in the aerodynamic calculation and the weight of the structure.

Acknowledgements

This work was carried out with the financial support of grant MK-398.2022.4 from the President of the Russian Federation.

References

1. Frenkel, J. The Viscosity of Liquids. Nature 125, 581–582 (1930).
2. Amosov, A. G. (2021). Classification indicators of maintainability of technical systems. AIP Conference Proceedings, 2402.
3. Amosov, A. G. (2021). Curvilinear trajectory of track machines. AIP Conference Proceedings, 2402.
4. Y. Solyaev, A. Babaytsev. Direct observation of plastic shear strain concentration in the thick GLARE laminates under bending loading. Composites Part B: Engineering, Vol. 224, 2021. Proceedings, 2402.
5. Pogodin V.A., Astapov A.N., Eremkina M.S., Babaytsev A.V., Rabinskiy L.N. Investigation of the low-temperature oxidation effect on the structure and mechanical properties of c/c composite. Nanoscience and Technology, Vol. 12, Issue 3, pp. 29 – 46, 2021, DOI: 10.1615/NanoSciTechnolIntJ.2021037997
6. Babaytsev A.V., Zotov A.A. Designing and Calculation of Extruded Sections of an Inhomogeneous Composition // Russian Metallurgy (Metally). Volume 2019, Issue 13, 1 December 2019, Pages 1452-1455, DOI: 10.1134/S0036029519130020
7. Pronina, P. F., Sun, Y., & Tushavina, O. V. (2020). Mathematical modelling of high-intensity heat flux on the elements of heat-shielding composite materials of a spacecraft. Journal of Applied Engineering Science, 18(4), 693-698.
8. Fedotenkov G., Rabinskiy, L., Lurie, S. Conductive Heat Transfer in Materials under Intense Heat Flows. Symmetrythis link is disabled, 2022, 14(9), 1950
9. Babaytsev, A.V., Astapov, A.N., Ripetskiy, A.V., Sha, M. Verification of mechanical properties and surface topography of PH1 stainless steel samples obtained by selective laser melting // Periodicals of Engineering and Natural Sciencesthis link is disabled, 2021, 9(4), pp. 417–432.
10. Orekhov, A. A., Rabinskiy, L. N., Fedotenkov, G. V., & Hein, T. Z. (2021). Heating of a half-space by a moving thermal laser pulse source. Lobachevskii Journal of Mathematics, 42(8), 1912-1919.
11. Kurbatov, A. S., Orekhov, A. A., Rabinskiy, L. N., Tushavina, O. V., & Kuznetsova, E. L. (2020). Research of the problem of loss of stability of cylindrical thinwalled structures under intense local temperature exposure. Periodico Tche Quimica, 17(34), 884-891.
12. Babaytsev A.V.; Kyaw Ye Ko; Vakhneev S. N.; Zin Hein Thant. Study of the influence of spherical inclusions on mechanical characteristics // Periodico Tche Quimica, (2020) vol. 17 (35) pp. 654-662.

13. A.V. Babaytsev; L.N. Rabinskiy; Kyaw Thu Aung. Investigation of the contact zone of a cylindrical shell located between two parallel rigid plates with a gap // Incas bulletin Volume 12 pp. 43 – 52. (2020)
14. Tushavina, O. V. (2020). Coupled heat transfer between a viscous shock gasdynamic layer and a transversely streamlined anisotropic half-space. INCAS Bulletin, 12(Special Issue), 211-220.
15. Babaytsev, A., Nikitin A., Ripetskiy A.. VHCF of the 3D-Printed Aluminum Alloy AlSi10Mg. Inventions 8(1):33, DOI:10.3390/inventions8010033
16. Babaytsev, A. V., Orekhov, A. A., & Rabinskiy, L. N. (2020). Properties and microstructure of AlSi10Mg samples obtained by selective laser melting. Nanoscience and Technology, 11(3), 213-222.
17. Thant Zin Hein, Arseniy V. Babaytsev, A.V. Ripetskiy. Effect of build atmosphere on the surface roughness of AlSi10Mg samples produced by selective laser melting // Nanoscience and Technology: An International Journal, 2022, Vol. 13, Issue 1, pp. 1-9.
18. N.A. Bulychev, L.N. Rabinskiy, O.V. Tushavina. Effect of Intensive Mechanic Vibration of Ultrasonic Frequency on Thermal Instable Low-Temperature Plasma, Nanoscience and Technology. An International Journal, 2020, Vol. 11, I. 1, pp. 15-21.
19. B.A. Garibyan. Enhancement of Mechanical Properties of Inorganic Glass under Ultrasonic Treatment, International Journal of Pharmaceutical Research, 2020, Vol. 12, Supplementary Issue 2, pp. 1829-1832.
20. M.O. Kaptakov. Effect of Ultrasonic Treatment on Stability of TiO2 Aqueous Dispersions in Presence of Water-Soluble Polymers, International Journal of Pharmaceutical Research, 2020, Vol. 12, Supplementary Issue 2, pp. 1821-1824.
21. O.A. Butusova. Surface Modification of Titanium Dioxide Microparticles Under Ultrasonic Treatment, International Journal of Pharmaceutical Research, 2020, Vol. 12, I. 4, pp. 2292-2296.
22. A.N. Tarasova. Vibration-based Method for Mechanochemical Coating Metallic Surfaces, International Journal of Pharmaceutical Research, 2020, Vol. 12, Supplementary Issue 2, pp. 1160-1168.
23. N.A. Bulychev. Study of Interaction of Surface-Active Polymers with ZnO Nanoparticles Synthesized in Ultrasonically Assisted Plasma Discharge, Nanoscience and Technology: An International Journal, 2022, Vol. 13, I. 1, pp. 55-65.
24. B.A. Garibyan. Mechanical Properties of Electroconductive Ceramics, International Journal of Pharmaceutical Research, 2020, Vol. 12, Supplementary Issue 2, pp. 1825-1828.
25. O.A. Butusova. Stabilization of Carbon Microparticles by High-Molecular Surfactants, International Journal of Pharmaceutical Research, 2020, Vol. 12, Supplementary Issue 2, pp. 1147-1151.
26. V. Goncharenko, Yu. Mikhaylov, N. Kartushina. Pattern recognition techniques for classifying aeroballistic flying vehicle paths, Neural Computing and Applications, 2022, Vol. 34, I. 5, pp. 4033-4045.
27. A.Yu. Burova. Theoretical basis, concept and methodology of control and correction of turbojet engines thrust asymmetry, Journal of Physics: Conference Series, 2022, 2308(1), 012006.
28. O.A. Butusova. Vinyl Ether Copolymers as Stabilizers of Carbon Black Suspensions, International Journal of Pharmaceutical Research, 2020, Vol. 12, Supplementary Issue 2, pp. 1152-1155.

29. M.O. Kaptakov. Catalytic Desulfuration of Oil Products under Ultrasonic Treatment, International Journal of Pharmaceutical Research, 2020, Vol. 12, Supplementary Issue 2, pp. 1838-1843.
30. A.N. Tarasova. Effect of Reagent Concentrations on Equilibria in Water-Soluble Complexes, International Journal of Pharmaceutical Research, 2020, Vol. 12, Supplementary Issue 2, pp. 1169-1172.
31. O.A. Butusova. Adsorption Behaviour of Ethylhydroxyethyl Cellulose on the Surface of Microparticles of Titanium and Ferrous Oxides, International Journal of Pharmaceutical Research, 2020, Vol. 12, Supplementary Issue 2, pp. 1156-1159.
32. A.N. Tarasova. Effect of Vibration on Physical Properties of Polymeric Latexes, International Journal of Pharmaceutical Research, 2020, Vol. 12, Supplementary Issue 2, pp. 1173-1180.
33. M.O. Kaptakov. Enhancement of Quality of Oil Products under Ultrasonic Treatment, International Journal of Pharmaceutical Research, 2020, Vol. 12, Supplementary Issue 2, pp. 1851-1855.
34. Y. Solyaev, A. Babaytsev. Direct observation of plastic shear strain concentration in the thick GLARE laminates under bending loading. Composites Part B: Engineering, Vol. 224, 2021. Proceedings, 2402.
35. Bodryshev, V.V., A.V., Orekhov, Babaytsev, A.A., Min, Y.N. Digital method for analysing speckle-interferometric images of material deformation. Periodicals of Engineering and Natural Sciences, 2021, 9(3), pp. 886–900.
36. Astapov, A., Rabinskiy, L., & Tushavina, O. (2021). Oxidation resistance of a si–tisi2–mosi2–tib2–casi2 coating on a cf/c–sic substrate in high-speed high-enthalpy air plasma flows. Nanomaterials, 11(10).
37. Astapov, A. N., Rabinskiy, L. N., Tushavina, O. V., & Starovoitov, E. I. (2021). Influence of air plasma flow on a cf /sic composite with a si-tisi2-mosi2-tib2-casi2 heat-resistant coating system. Journal of the Balkan Tribological Association, 27(2), 231-242.